



City Research Online

City St George's, University of London

Citation: White, M., Oyewunmi, O. A., Chatzopoulou, M. T., Pantaleo, A. M., Haslam, A. J. & Markides, C. N. (2017). Integrated computer-aided working-fluid design and thermoeconomic ORC system optimisation. *Energy Procedia*, 129, pp. 152-159. doi: 10.1016/j.egypro.2017.09.095

This is the published version of the paper.

This version of the publication may differ from the final published version. To cite this item please consult the publisher's version.

Permanent repository link: <https://openaccess.city.ac.uk/id/eprint/19978/>

Link to published version: <https://doi.org/10.1016/j.egypro.2017.09.095>

Copyright and Reuse: Copyright and Moral Rights remain with the author(s) and/or copyright holders. Copies of full items can be used for personal research or study, educational, or not-for-profit purposes without prior permission or charge, unless otherwise indicated, provided that the authors, title and full bibliographic details are credited, a hyperlink and/or URL is given for the original metadata page and the content is not changed in any way. For full details of reuse please refer to [City Research Online policy](#).



IV International Seminar on ORC Power Systems, ORC2017
13-15 September 2017, Milano, Italy

Integrated computer-aided working-fluid design and thermoeconomic ORC system optimisation

M. T. White^a, O. A. Oyewunmi^a, M. A. Chatzopoulou^a, A. M. Pantaleo^{a,b}, A. J. Haslam^a,
C. N. Markides^{a,*}

^a*Clean Energy Processes (CEP) Laboratory, Department of Chemical Engineering,
Imperial College London, South Kensington Campus, London, SW7 2AZ, UK*

^b*Department of Agro-environmental Sciences, University of Bari, Via Amendola 165/A 70125, Bari, Italy*

Abstract

The successful commercialisation of organic Rankine cycle (ORC) systems across a range of power outputs and heat-source temperatures demands step-changes in both improved thermodynamic performance and reduced investment costs. The former can be achieved through high-performance components and optimised system architectures operating with novel working-fluids, whilst the latter requires careful component-technology selection, economies of scale, learning curves and a proper selection of materials and cycle configurations. In this context, thermoeconomic optimisation of the whole power-system should be completed aimed at maximising profitability. This paper couples the computer-aided molecular design (CAMD) of the working-fluid with ORC thermodynamic models, including recuperated and other alternative (e.g., partial evaporation or trilateral) cycles, and a thermoeconomic system assessment. The developed CAMD-ORC framework integrates an advanced molecular-based group-contribution equation of state, SAFT- γ Mie, with a thermodynamic description of the system, and is capable of simultaneously optimising the working-fluid structure, and the thermodynamic system. The advantage of the proposed CAMD-ORC methodology is that it removes subjective and pre-emptive screening criteria that would otherwise exist in conventional working-fluid selection studies. The framework is used to optimise hydrocarbon working-fluids for three different heat sources (150, 250 and 350 °C, each with $\dot{m}c_p = 4.2$ kW/K). In each case, the optimal combination of working-fluid and ORC system architecture is identified, and system investment costs are evaluated through component sizing models. It is observed that optimal working fluids that minimise the specific investment cost (SIC) are not the same as those that maximise power output. For the three heat sources the optimal working-fluids that minimise the SIC are isobutane, 2-pentene and 2-heptene, with SICs of 4.03, 2.22 and 1.84 £/W respectively.

© 2017 The Authors. Published by Elsevier Ltd.

Peer-review under responsibility of the scientific committee of the IV International Seminar on ORC Power Systems.

Keywords: organic Rankine cycle; ORC; computer-aided molecular-design; CAMD; group contribution; SAFT- γ Mie; technoeconomic optimisation.

1. Introduction

The working fluid used within an organic Rankine cycle (ORC) can affect performance, component design, size, cost and operational procedures. However, with increasing concerns over global warming and air pollution, certain

* Corresponding author. Tel.: +44 (0)20 759 41601.

E-mail address: c.markides@imperial.ac.uk

Nomenclature

A_c, A_h	condenser/evaporator area, m ²
C_n	number of Carbon atoms
c_p	specific heat capacity, J/(kg K)
C_p^0	component cost, £
F	material factor
P_2	evaporation pressure, Pa
P_{cr}	critical pressure, Pa
P_r	reduced pressure
PP_c, PP_h	condenser and evaporator pinch points, K
SIC	specific investment cost, £/W
T_1	condensation temperature, K
T_3'	temperature at end of evaporation, K
T_{hi}, T_{ci}	heat-source and heat-sink inlet temperatures, K
Z	cost coefficient
X	sizing attribute
η_p, η_e	pump and expander isentropic efficiencies
\dot{m}	mass flow rate, kg/s
$\dot{W}_p, \dot{W}_e, \dot{W}_n$	pump, expander and net power output, W
ΔT_{sh}	amount of superheating, K

fluids such as CFCs have already been phased out, whilst fluids such as HCFCs and HFCs are set to be phased out in the coming years. From the perspective of an end-user, technical solutions are required that are not constrained by such legislation, in addition to being economically feasible. This demands the identification of both novel working fluids that meet all legislated requirements, and ORC systems that are optimised in terms of performance indicators such as the net-present value or the levelised cost of energy.

Compared to conventional working-fluid selection studies, in which a group of fluids are screened based on predefined criteria after which parametric optimisation studies are performed, computer-aided molecular design (CAMD) can be used to simultaneously optimise the working fluid and the ORC system. CAMD-ORC models have the potential to identify novel working-fluids which may otherwise be overlooked, whilst removing preemptive and subjective screening criteria. Papadopoulos et al. [1] used CAMD to identify potential working-fluid candidates before completing a more conventional ORC process simulation, and later applied CAMD to the optimal design of working-fluid mixtures [2]. Brignoli and Brown [3] used group-contribution methods to investigate the effect of a working-fluid's critical point on the thermodynamic performance of the ORC, whilst Palma-Flores et al. [4] demonstrated the potential of CAMD to identify new fluids with higher thermal efficiencies and better safety characteristics. Furthermore, Su and Deng [5] developed a thermodynamic ORC model, intended for future application within a CAMD-ORC framework. However, these previous studies have relied on empirical group-contribution methods. More advanced group-contribution equations of state have also been applied within a CAMD-ORC framework. For example, Lampe et al. [6,7] optimised ORC systems for a geothermal application. The CAMD-ORC optimisation was split into two stages. In the first stage an optimal, but hypothetical, working fluid was identified, and in the second stage real working fluids with similar performance were identified. More recently, Schilling et al. [8] reduced the problem to a single stage optimisation in which the working-fluid structure and ORC system are simultaneously optimised.

The major limitation of previous CAMD-ORC models is a focus on optimising the thermodynamic cycle; however, achieving the successful commercialisation of ORC systems across a range of applications requires a consideration thermoeconomic performance. Quoilin et al. [9] evaluated the specific-investment cost (SIC) of small-scale waste-heat driven ORC units, whilst Lecompte et al. [10] optimised the design of ORC units for large-scale CHP plants and waste-heat recovery. Multi-objective optimisation studies can be also found in the literature [11–13], where the authors considered the trade-off between maximising power output whilst minimising the SIC. However, all of these previous thermoeconomic studies consider only predefined working fluids, and conduct a separate optimisation for each specific fluid. On the contrary, thermoeconomic methods have not been previously applied to CAMD-ORC

models, partly due to the requirement of group-contribution methods for determining transport properties to size the system components.

The aim of this study is to combine group-contribution methods for transport properties, component sizing models, and thermoeconomic analysis into an existing CAMD-ORC framework based on SAFT- γ Mie [14]. So far as the authors are aware, this is the first known attempt to couple a CAMD-ORC model, based on an advanced group-contribution equation of state, with a thermoeconomic assessment in this manner. In Section 2 the key aspects the CAMD-ORC framework are discussed. In Section 3 the framework is applied to a case study considering the design of hydrocarbon working fluids. Finally, the key findings from this study are discussed in Section 4.

2. CAMD-ORC model

2.1. Group-contribution methods

Group-contribution methods determine the properties of a particular molecule based on the functional groups that make it up. For example, isopentane is described by three $-\text{CH}_3$ groups, one $-\text{CH}_2$ and one $>\text{CH}-$ group. In a group-contribution method group parameters are only required for the individual groups, which allows the evaluation of novel working fluids for which property prediction would not be possible using conventional approaches. To capture the trade-off between thermodynamic performance and system costs, group-contribution methods are required for both the thermodynamic properties and transport properties. In this work, the SAFT- γ Mie equation of state [15] is used for thermodynamic property prediction. SAFT- γ Mie a state-of-the-art version of statistical associating fluid theory (SAFT) [16,17] wherein a Mie potential is used to model the interaction between two molecular groups [15]. Group parameters are available for the hydrocarbon groups considered within this paper, and have been validated against experimental data [18]. Unfortunately, SAFT is only suitable for determining thermodynamic properties, so alternative methods are required for the transport properties. Previously, empirical group-contribution methods for the prediction of transport properties have been applied to hydrocarbon working fluids, and validated against data from NIST [14]. The correlations applied here are summarised in Ref. [14].

2.2. Thermodynamic modelling

The thermodynamic analysis of the ORC is well described within the literature, and consists of applying an energy balance to each component with the cycle. Besides analysing a sub-critical, non-recuperated cycle, the CAMD-ORC model can also be used to evaluate cycles operating with mixtures, recuperated cycles, and cycles with partial evaporation. For a mixture both working fluids are described by their functional groups and the variable x is introduced to represent the mass fraction of the first fluid. A recuperated cycle is modelled by a fixed recuperator effectiveness ϵ_r , and the inclusion of a recuperator is defined by a binary flag. Finally, partially-evaporated cycles are modelled by defining one optimisation variable, z , which can describe both partially-evaporated and superheated cycles, and varies between 0 and 2. When $0 \leq z \leq 1$, two-phase expansion is assumed and z is equal to the expander inlet vapour quality. When $1 < z \leq 2$, the working fluid expands from a superheated state and the amount of superheating ΔT_{sh} is given by:

$$\Delta T_{\text{sh}} = (z - 1)(T_{\text{hi}} - T_{3'}), \quad (1)$$

where T_{hi} is the heat-source inlet temperature and $T_{3'}$ is the saturated-vapour temperature. In all cycles, the condensation temperature T_1 , reduced pressure P_r (P_2/P_{cr} , where P_2 and P_{cr} are the evaporation and critical pressures respectively), pump efficiency η_p and expander efficiency η_e are defined. The working-fluid mass flow rate is determined by the evaporator pinch point PP_{h} , whilst the minimum condenser pinch point $PP_{\text{c,min}}$ is defined as a constraint.

2.3. Component sizing and thermoeconomic analysis

The evaporator and condenser are assumed to be tube-in-tube heat exchangers (HEX), which are cost effective for small- to medium-scale applications. The HEXs are sized by determining the total required heat-transfer area, which is obtained by calculating the heat-transfer coefficient (HTC) in the different single- and two-phase HXC heat-transfer regions. In the evaporator this corresponds to single-phase preheating, two-phase evaporation and single-phase superheating regions, and in the condenser it corresponds to single-phase precooling and two-phase condensation regions.

Depending on the heat-transfer region, different Nusselt-number correlations are applied to determine the local HTC. For single-phase heat transfer the Dittus-Boelter [19] correlation has been used. For evaporation, the correlations

proposed by Cooper [20] and Gorenflo [21] have been used for nucleate-boiling conditions, whereas the Dobson [22] and Zuber [20] correlations have been used to account for the convective-heat-transfer phenomena. For condensation inside tubes, the correlations proposed by Shah [23] and Dobson [22] have been considered, accounting for both gravity driven and shear driven condensation. The reader can refer to Ref. [24] for a detailed analysis and comparison of the correlations selected. The Nusselt-number correlations for two-phase heat transfer are typically a function of the vapour quality, which varies along the length of the HEX. Therefore, the HEX length is discretised into n segments. For each segment the vapour quality is assumed to be constant and an estimate for the heat-transfer area for that segment is obtained. The total heat-transfer area is simply the summation of all the segments. Pressure drops within the heat exchangers are neglected, however, the HEX tubes are sized to maintain a liquid flow velocity of 1.5–3 m/s, which is in line with good practice industry standards aimed at minimising pressure drops.

Since there are only a limited number of ORC applications worldwide, and system cost data are not publicly available, cost correlations originating from the chemical industry are commonly used in the literature. A well-established method is the module costing technique [25], which provides the costs of individual components, based on a specific sizing attribute (*e.g.*, heat-transfer area for HEXs, *etc.*). By adding the individual component costs the total ORC unit cost is obtained. The costing method applied within this study is summarised in Ref. [24] and uses the cost correlations given by Seider et al. [26]:

$$C_p^0 = F \exp(Z_1 + Z_2 \ln(X) + Z_3 \ln(X)^2 + Z_4 \ln(X)^3 + Z_5 \ln(X)^4), \quad (2)$$

and Turton et al. [27]:

$$C_p^0 = F 10^{(Z_1 + Z_2 \log(X) + Z_3 \log(X)^2)}, \quad (3)$$

where C_p^0 is the component cost in £; F is a material factor accounting for the component manufacturing; Z_i is the cost coefficient; and X is the sizing attribute. Both Z_i and X vary depend on the type of the equipment selected and the values used to estimate the purchase cost of each piece of equipment are summarised in Table 1. It is assumed that the pump is a centrifugal pump, whilst the heat exchangers are of tube-in-tube construction. The expander is assumed to be a radial turbine, and this component's cost is based only on the power output. In reality, the pressure ratio across the expander will impact both the expander efficiency and cost. Within this work these effects have been neglected owing to the complexities of requiring a more detailed expander model, and because correlations that consider these effects are either not currently available, or not sufficiently validated. However, these effects should be considered in future studies. Finally, the Chemical Engineering Plant Cost Index (CEPCI) is used to convert the cost to today's values. For Turton et al. [27] the basis year is 2001 ($\text{CEPCI}_{2001} = 397$), whilst for Seider et al. [26] the basis year is 2006 ($\text{CEPCI}_{2006} = 500$). The costs are converted to today's values using $\text{CEPCI}_{2016} = 556.8$.

Table 1. Cost correlations coefficients

Component	Attribute (X)	F	Z_1	Z_2	Z_3	Z_4	Z_5	Ref.
Expander	Power, \dot{W}_e (kW)	3.5	2.2486	1.4965	-0.1618	0	0	[27]
Pump	S^*	2.7	9.2951	-0.6019	0.0519	0	0	[26]
Pump motor	Power, \dot{W}_p (HP)	1.4	5.83	0.134	0.0533	0.0286	0.00355	[26]
Evaporator - Condenser	Area (m^2)	1	9.5638	0.532	-0.0002	0	0	[26]
Preheater - Desuperheater	Area (m^2)	1	10.106	-0.4429	0.0901	0	0	[26]

* $S = \dot{V} \sqrt{H}$ where \dot{V} is the pump volumetric flow rate in gallons per minute and H is the pump head in feet.

2.4. Optimisation

The CAMD-ORC framework is formulated in gPROMS [28], and the optimisation is completed using the OAERAP outer-approximation algorithm. The optimisation concerns integer variables describing the working-fluid molecular structure and continuous variables describing the power system, and therefore is a mixed-integer non-linear programming (MINLP) problem. The optimisation is solved by first relaxing the integer variables to continuous variables and completing a non-linear programming (NLP) optimisation, which in turn supplies a maximum for the objective function. The MINLP is then solved by successive iterations of a mixed-integer linear programming problem (MILP), in which the objective function and constraints are linearised, and an additional NLP in which the power system variables are optimised for a particular fluid identified from the MILP.

3. Case study

The CAMD-ORC framework has previously been used to optimise the working fluid and thermodynamic cycle for three different waste-heat streams [14]. Furthermore, the transport-property group-contribution correlations have been coupled to the heat-exchanger sizing model, and the heat-transfer area requirements for a few of the optimal cycles that resulted from the initial thermodynamic study have been determined [29]. The current study aims to determine the heat-transfer requirements for a larger group of working-fluids, and determine the total specific investment cost (SIC) for each working-fluid. This, in turn, allows optimal cycle configurations to be identified based on thermoeconomics. The three heat-sources are each defined by a heat-capacity rate ($\dot{m}c_p$) of 4.2 kW/K, and are defined at 150, 250 and 350 °C respectively. The assumptions for the study are listed in Table 2, whilst the working-fluids under consideration are given in Table 3. The heat-source is the heat-transfer oil Therminol 66 at 1 bar, and the heat-sink is water.

Table 2. Assumptions for the ORC thermodynamic study completed in Ref. [14].

$(\dot{m}c_p)_h$ W/K	T_{ci} °C	$c_{p,c}$ J/(kg K)	\dot{m}_c kg/s	η_p %	η_e %	$PP_{c,min}$ °C	$P_{1,min}$ bar
4200	15	4200	5.0	70	80	5	0.25

Table 3. Working-fluid groups considered within this study.

<i>n</i> -alkanes	methyl alkanes	1-alkenes	2-alkenes
$\text{CH}_3-(\text{CH}_2)_n-\text{CH}_3$	$(\text{CH}_3)_2-\text{CH}-(\text{CH}_2)_n-\text{CH}_3$	$\text{CH}_2=\text{CH}-(\text{CH}_2)_n-\text{CH}_3$	$\text{CH}_3-\text{CH}=\text{CH}-(\text{CH}_2)_n-\text{CH}_3$

For each working-fluid group in Table 3 a parametric study was completed whereby the number of $-\text{CH}_2$ groups was varied, and the ORC thermodynamic variables were optimised to maximise the power output from the system [14]. For this study a sub-critical, non-recuperated cycle was assumed, owing to the assumptions that adding a recuperator to system does not result in a higher power output, and that partial-evaporation cycles require expanders capable of handling two-phase fluids which are still at an early stage of development and therefore no cost data are available. The results from this parametric study are plotted in terms of the power output in Figure 1; here C_n refers to the number of carbon atoms in the molecule (*n*-alkane, methyl alkane, 1-alkene or 2-alkene). Furthermore, for each optimal cycle shown in Figure 1, the required heat-transfer areas for the evaporator and condenser were obtained using the heat-exchanger sizing model based on the group-contribution transport properties (Figure 2).

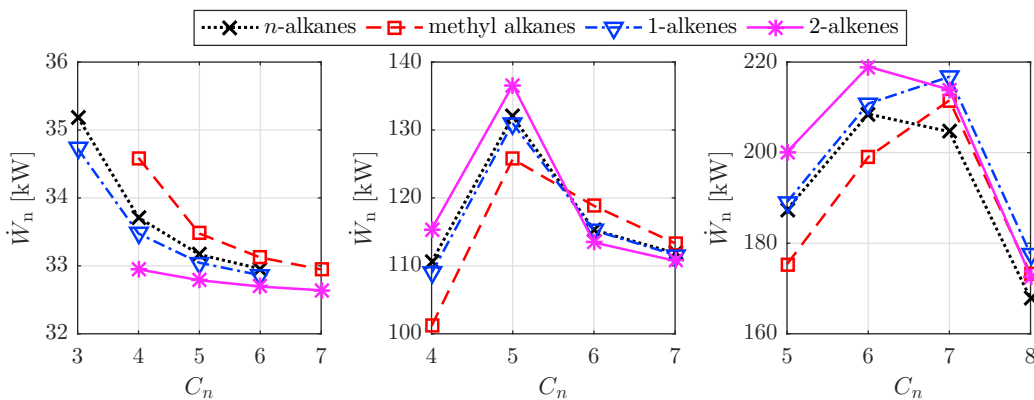


Fig. 1. Optimal net power output from an ORC system operating with different hydrocarbon working fluids. Results are plotted against the number of Carbon atoms C_n in the molecule (*n*-alkane, methyl alkane, 1-alkene or 2-alkene, as indicated). From left to right: $T_{hi} = 150, 250, 350$ °C.

In terms of the power output, the optimal working fluids for the three-heat sources are *n*-propane, 2-pentene and 2-hexene, corresponding to maximum power outputs of 35.2, 136.7 and 219.0 kW respectively. For the 150 and 250 °C heat-sources, the optimal cycles also result in the largest heat exchangers. The reason for this is explored in Figure 3, in which are displayed three of the cycles ($C_n = 4, 5$ and 6) for the *n*-alkane, 250 °C case-study on a

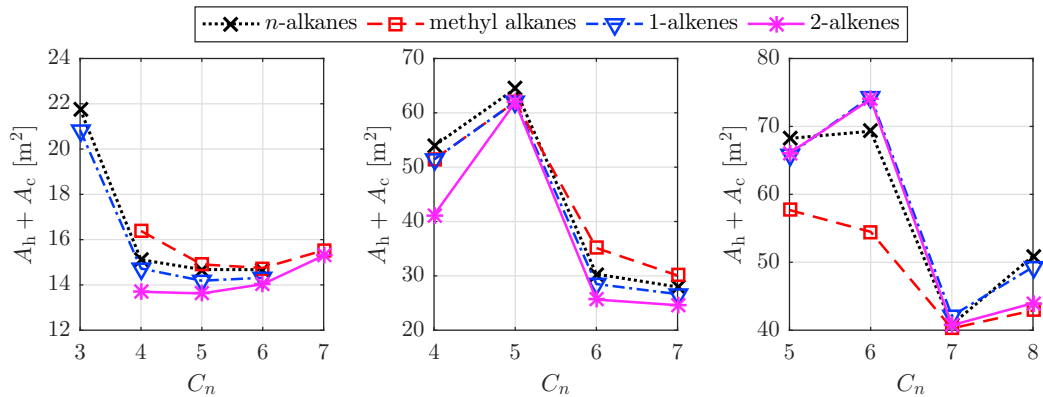


Fig. 2. Total heat-transfer area requirements for each cycle previously identified in Figure 1. From left to right: $T_{hi} = 150, 250, 350$ °C.

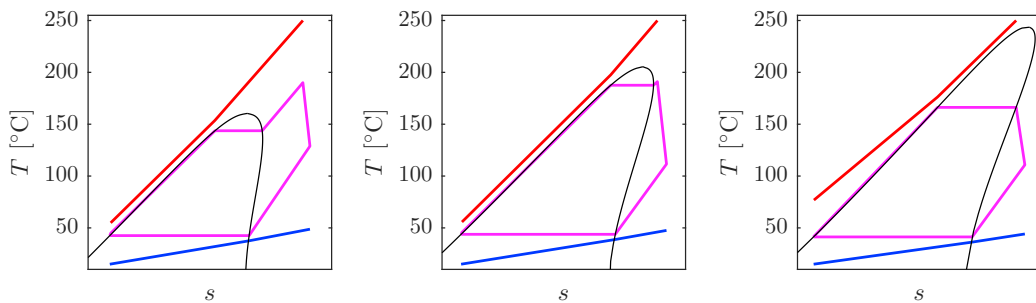


Fig. 3. T - s plots for three cycles from the n -alkane, 250 °C case-study. From left to right: $C_n = 4$ (n -butane), 5 (n -pentane) and 6 (n -hexane). The red and blue lines are the heat-source and heat-sink streams, the magenta lines are the ORC and the black line is the working-fluid saturation dome.

T - s diagram. When $C_n = 4$, the evaporation pressure is constrained by the critical temperature, which results in an optimal cycle with a high reduced-pressure and a large amount of superheating. This reduces the power output from the system and reduces the evaporator area because of the increased temperature difference between the heat-source and working-fluid in the evaporation and superheating regions. In comparison, when $C_n = 6$, the evaporation pressure is constrained by the heat-source temperature, which results in a large latent heat of vaporisation. This again increases the temperature difference within the evaporator and reduces the heat-transfer area requirements. However, where $C_n = 5$, the optimal cycle has a high reduced pressure but minimal superheating. This results in a low latent heat of vaporisation, and consequently a large amount of heat-transfer occurring in the preheating region. This is favourable in terms of maximising the power output, but also results in a large evaporator heat-transfer area.

Considering the 350 °C heat source, the relationship between the maximum power and the maximum heat-transfer area is not as clear. While 2-hexene results in the highest power output, and largest heat-exchanger area, moving to 1-hexene results in a similar power output, but a significantly smaller heat-transfer-area requirement. This can be explained by considering the condensation conditions within these cycles. Since the saturation temperature at atmospheric pressure increases as molecular complexity increases, and because a minimum condensation pressure constraint is applied (0.25 bar), the resulting cycles for the more complex molecules result in higher condensation temperatures. A higher condensation temperature increases the minimum allowable heat-source temperature, which in turn moves the evaporator pinch-point to the preheating inlet, rather than at the start of evaporation. This increases the temperature difference between the heat-source and working-fluid in both the preheating and evaporation regions. Furthermore, the higher condensation temperature also increases the temperature difference between the heat-sink and working-fluid. These effects can lead to a large reduction in heat-transfer area, as observed in Figure 2 for $C_n = 7$.

Clearly, there is a trade-off between thermodynamic performance and the size of the system components. Using the known heat-transfer areas, the pump work and expander work for each cycle, the cost correlations described in Section 2.3 can be used to obtain the specific investment cost (SIC) (Figure 4). As one would expect, the smallest systems (150 °C) correspond to highest SIC whilst the largest systems (350 °C) correspond to the lowest SIC. This is partly

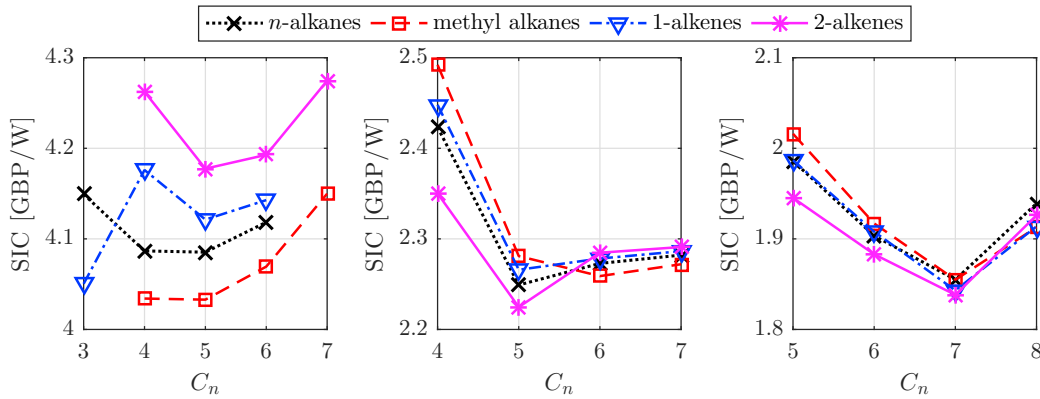


Fig. 4. Specific investment cost (SIC) in £/W for each optimal cycle previously identified in Figure 1. From left to right: $T_{hi} = 150, 250, 350$ °C.

attributable to the higher relative costs associated with manufacturing smaller components, and partly attributable to the inherent lower efficiencies as the heat-source temperature reduces.

More interestingly though, for each heat-source temperature and hydrocarbon family, except the 1-alkene, 150 °C case study, there appears to be a particular working fluid that will minimise the SIC. For the 150, 250 and 250 °C heat-source temperatures the minimum SICs are 4.03, 2.22 and 1.84 £/W respectively, and these are found for $C_n = 4$ (isobutane), $C_n = 5$ (2-pentene) and $C_n = 7$ (2-heptene) respectively. For the 250 °C heat source 2-pentene is found to both maximise the power output and minimise the SIC, and is therefore identified as the optimal working fluid. However, for the other two heat sources, different working fluids are identified based on whether a thermodynamic or techno-economic performance metric is used. In particular, for the 350 °C heat source, the results suggest that in terms of minimising the SIC, it could be beneficial to use a working fluid with a relatively high condensation temperature, as this increases the temperature difference within the evaporator and reduces the heat-transfer area requirement.

The discrepancy observed for the 1-alkene, 250 °C case study is due to a very large superheating. This results in a high expander outlet temperature, which in turn results in a higher desuperheater load, but also results in a lower condenser load. However, a high temperature difference within the desuperheater is also observed which results in only a small rise in the heat-transfer area, and a less significant increase in the condenser cost compared to the *n*-alkane, 150 °C case study. Overall, the result of this is a reduction in the SIC, as observed in Figure 4 for $C_n = 3$.

4. Conclusions

The discovery of new working-fluids that meet increasingly restrictive environmental legislation, and the identification of optimal ORC systems based on techno-economic performance indicators are key steps to enable a more widespread uptake of ORC technology. The aim of this paper has been to incorporate techno-economic analysis, through component sizing and suitable cost correlations, into an existing CAMD-ORC framework based on the SAFT- γ Mie equation of state. Heat exchanger sizing models, based on group-contribution methods for determining transport properties, have been used to size the evaporator and condenser for optimised ORC systems, and the resulting specific investment costs (SIC) have been determined for three different case studies. It is found that working fluids that maximise the power output from the system generally have the highest heat-exchanger area requirements. Therefore, working-fluid selection based on SIC minimisation can result in different optimal working fluids to those identified from an optimisation that considers power output or other common thermodynamic objective functions. For the three heat-sources temperatures considered (150, 250 and 350 °C, each with $\dot{m}_{c_p} = 4.2$ kW/K) the three working fluids that minimise the SIC are isobutane, 2-pentene and 2-heptene, with SICs of 4.03, 2.22 and 1.84 £/W respectively. The corresponding power outputs for these systems are 33.5, 136.6 and 213.9 kW, and these power outputs are 4.9%, 0.0% and 2.3% lower than the power outputs obtained for working fluids that maximise the power output. Overall, the results have demonstrated the importance of considering techno-economic performance within the CAMD-ORC framework, and three optimal working have been identified for different heat-source temperatures. The next steps are to include the sizing models within the optimisation framework and to conduct a multi-objective optimisation to investigate the cost/benefit balance, in addition to investigating investment profitability and the effect of different operational strategies on the global energy conversion efficiencies and revenues generated from the system.

Acknowledgements

This work was supported by the UK Engineering and Physical Sciences Research Council (EPSRC) [grant number EP/P004709/1]. The authors would like to thank the Imperial College Presidents PhD Scholarship Scheme, and the Climate-KIC PhD Added Programme for funding this research. Data supporting this publication can be obtained on request from cep-lab@imperial.ac.uk.

References

- [1] Papadopoulos, A.I., Stijepovic, M., Linke, P. On the systematic design and selection of optimal working fluids for organic Rankine cycles. *Appl Therm Eng* 2010;30(6-7):760–769.
- [2] Papadopoulos, A.I., Stijepovic, M., Linke, P., Seferlis, P., Voutetakis, S. Toward optimum working fluid mixtures for organic Rankine cycles using molecular design and sensitivity analysis. *Ind Eng Chem Res* 2013;52(34):12116–12133.
- [3] Brignoli, R., Brown, J.S.. Organic Rankine cycle model for well-described and not-so-well-described working fluids. *Energy* 2015;86:93–104.
- [4] Palma-Flores, O., Flores-Tlacuahuac, A., Canseco-Melchorb, G.. Simultaneous molecular and process design for waste heat recovery. *Energy* 2016;99:32–47.
- [5] Su, W., Zhao, L., Deng, S.. Developing a performance evaluation model of organic Rankine cycle for working fluids based on the group contribution method. *Energy Convers Manage* 2017;132:307–315.
- [6] Lampe, M., Stavrou, M., Buckner, H.M., Gross, J., Bardow, A.. Simultaneous optimization of working fluid and process for organic Rankine cycles using PC-SAFT. *Ind Eng Chem Res* 2014;53(21):8821–8830.
- [7] Lampe, M., Stavrou, M., Schilling, J., Sauer, E., Gross, J., Bardow, A.. Computer-aided molecular design in the continuous-molecular targeting framework using group-contribution PC-SAFT. *Comput Chem Eng* 2015;81:278–287.
- [8] Schilling, J., Lampe, M., Gross, J., Bardow, A.. 1-stage CoMT-CAMD: An approach for integrated design of ORC process and working fluid using PC-SAFT. *Chem Eng Sci* 2017;159:217–230.
- [9] Quoilin, S., Declaye, S., Tchanche, B.F., Lemort, V.. Thermo-economic optimization of waste heat recovery organic Rankine cycles. *Appl Therm Eng* 2011;31(14):2885–2893.
- [10] Lecompte, S., Huisseune, H., van den Broek, M., De Schamphelaere, S., De Paepe, M.. Part load based thermo-economic optimization of the organic Rankine cycle (ORC) applied to a combined heat and power (CHP) system. *Appl Energy* 2013;111:871–881.
- [11] Oyewunmi, O.A., Markides, C.N.. Thermo-economic and heat transfer optimization of working-fluid mixtures in a low-temperature organic Rankine cycle system. *Energies* 2016;9:448.
- [12] Andreasen, J.G., Kaern, M.R., Pierobon, L., Larsen, U., Haglund, F.. Multi-objective optimization of organic Rankine cycle power plants using pure and mixed working fluids. *Energies* 2016;9:322.
- [13] Feng, Y., Hung, T., Zhang, Y., Li, B., Yang, J., Shi, Y.. Performance comparison of low-grade ORCs (organic Rankine cycles) using R245fa, pentane and their mixtures based on the thermoeconomic multi-objective optimization and decision makings. *Energy* 2015;93:2018–2029.
- [14] White, M.T., Oyewunmi, O.A., Haslam, A.J., Markides, C.N.. High-efficiency industrial waste-heat recovery through computer-aided integrated working-fluid and ORC system optimisation. *Energy Convers Manage* ; accepted manuscript.
- [15] Papaioannou, V., Lafitte, T., Avendaño, C., Adjiman, C.S., Jackson, G., Müller, E.A., et al. Group contribution methodology based on the statistical associating fluid theory for heteronuclear molecules formed from Mie segments. *J Chem Phys* 2014;140(5):1–29.
- [16] Chapman, W.G., Gubbins, K.E., Jackson, G., Radosz, M.. SAFT: Equation-of-state solution model for associating fluids. *Fluid Phase Equilib* 1989;52:31–38.
- [17] Chapman, W.G., Gubbins, K.E., Jackson, G., Radosz, M.. New reference equation of state for associating liquids. *Ind Eng Chem Res* 1990;29(8):1709–1721.
- [18] Dufal, S., Papaioannou, V., Sadeqzadeh, M., Pogiatis, T., Chremos, A., Adjiman, C.S., et al. Prediction of thermodynamic properties and phase behavior of fluids and mixtures with the SAFT- γ Mie group-contribution equation of state. *J Chem Eng Data* 2014;59(10):3272–3288.
- [19] Bergman, T.L., Lavine, A.S., Incropera, F.P., DeWitt, D.P.. *Fundamentals of Heat and Mass Transfer*. John Wiley & Sons; 2011.
- [20] Hewitt, G.F., Shires, G.L., Bott, T.R.. *Process heat transfer*. CRC Press; 1994.
- [21] Verein Deutscher Ingenieure, . *VDI Heat Atlas*. Second ed.; Springer; 2010.
- [22] Dobson, M.K., Wattelet, J.P., Chato, J.C.. Optimal sizing of two-phase heat exchangers. *Tech. Rep.*; 1993.
- [23] Shah, M.. A general correlation for heat transfer during film condensation inside pipes. *Int J Heat Mass Transf* 1979;22(4):547–556.
- [24] Chatzopoulou, M.A., Markides, C.N.. Advancements in organic Rankine cycle system optimisation for combined heat and power applications: Components sizing and thermoeconomic considerations. In: 30th International Conference on Efficiency, Cost, Optimization, Simulation and Environmental Impact of Energy Systems. 2-6th July, San Diego, California, USA; 2017..
- [25] Lemmens, S.. Cost engineering techniques and their applicability for cost estimation of organic Rankine cycle systems. *Energies* 2016;9(7).
- [26] Seider, W., Seader, J., Lewin, D.. *Product and Process Design Principles - Synthesis, Analysis, and Evaluation*. Second ed.; John Wiley & Sons, Inc., Hoboken, New Jersey; 2009. ISBN 978-0470-048-5.
- [27] Turton, R., Bailie, R.C., Whiting, W.B., Shaelwitz, J.A.. *Analysis, Synthesis and Design of Chemical Processes*; vol. 53. Third ed.; Pearson Education, Inc., Boston, MA 02116; 2009.
- [28] Process Systems Enterprise Ltd., . gPROMS. 2017. URL: <http://www.psenterprise.com>.
- [29] Oyewunmi, O.A., White, M.T., Chatzopoulou, M.A., Haslam, A.J., Markides, C.N.. Integrated computer-aided working-fluid design and power system optimisation: Beyond thermodynamic modelling. In: 30th International Conference on Efficiency, Cost, Optimization, Simulation and Environmental Impact of Energy Systems. 2-6th July, San Diego, California, USA; 2017..